An Improved Shear Lag Model for Broken Fibers in Composite Materials

C. M. LANDIS, M. A. MCGLOCKTON AND R. M. MCMEEKING*
Department of Mechanical and Environmental Engineering
University of California, Santa Barbara
Santa Barbara, CA 93106

(Received November 5, 1997)
(Revised April 30, 1998)

ABSTRACT: A shear lag model is formulated to predict the stresses in a unidirectional fiber reinforced composite. The model is based on assumptions consistent with the finite element method and the principle of virtual work by assuming that the matrix displacements can be interpolated from the fiber displacements. The fibers are treated as one-dimensional springs and the matrix is modeled as three-dimensional finite elements. The resulting finite element equations for the system are transformed into differential equations by taking the discretization length to approach zero. The governing ordinary differential equations are solved using Fourier transformations and an influence function technique. The technique is used to solve for the stresses around a single fiber break in an infinite square or hexagonal array of fibers. The results are compared with previous shear lag models and finite element results. The model predicts stress concentrations that are in good agreement with more detailed finite element analyses.

INTRODUCTION

Shear lag models have been used extensively for composite microstress analysis. Hedgepeth [1] and Hedgepeth and van Dyke [2], (HVD), calculated stress concentrations around clusters of broken fibers utilizing shear lag methodology. The two-dimensional analysis of Reference [1], representing layered composites, has been shown to be in good agreement with continuum elasticity solutions by Beyerlein et al. [3]. On the other hand, the three-dimensional model of Hedgepeth and van Dyke [2] does not agree with some more detailed finite element calculations done by Nedele and Wisnom [4,5].

*Author to whom correspondence should be addressed.

0021-9983/99/07 0667–14 $10.00/0

Cox [6] introduced the shear lag concept by formulating a model to determine the stresses in a broken fiber embedded in a composite. Hedgepeth and van Dyke [2], (HVD), extended the model to account for the stresses in all other fibers in the composite. Sastry and Phoenix [7] then used the two-dimensional version of the model [1] to develop the break influence superposition techniques (BIS), which allows the stresses to be determined at any location in a composite given the locations of multiple fiber fractures. Beyerlein and Phoenix [8] have used BIS to study the fracture and strength properties of two-dimensional layered composites.

The shear lag models of HVD assume an infinite array of fibers. For a three-dimensional system, the array can be square or hexagonal. The fibers are approximated as one-dimensional, axial load carrying entities. The fibers are allowed to displace only in the axial direction and transverse displacements are not considered in the model. The matrix is assumed to carry no axial load, and its only role is to transfer load between fibers via shear stresses. In the HVD model, the matrix is approximated by a continuous distribution of linear shear springs connecting any given fiber to its nearest neighbors only. For square and hexagonal arrays this implies that there are four and six connections per fiber respectively. Equilibrium of forces in each fiber yields an infinite set of coupled, linear, ordinary differential equations governing the axial displacements of the fibers. A Fourier series transformation is applied to these equations to yield a single ordinary differential equation. The resulting differential equation is solved in transformed space and then the inverse Fourier transformation is applied to yield the influence function required to evaluate the stresses in the fibers in real space.

A difficulty with the HVD model lies in the representation of the matrix. The original HVD paper makes use of a quantity h/d which is essentially undefined, but purports to represent the ratio of fiber thickness, h, to fiber spacing, d. Hedgepeth and van Dyke claim that the effective matrix shear stiffness per unit thickness is $G_m h/d$, where G_m is the axial shear modulus of the matrix. In reality, the axial shear stiffness per unit thickness of a slab of elastic matrix with a square plan form is always G_m and therefore, the quantity h/d must be equal to unity for consistency. The results show that the quantity h/d has no effect on the stress concentrations in the HVD model but it does influence the lengths of fiber segments over which stress concentrations appear. Our deduction is that h/d should be set to unity to provide physically consistent spring stiffnesses to represent a square section of matrix with axial shear modulus G_m. The HVD model also neglects direct interactions of fibers with their next nearest neighbors. This assumption does have profound effects on the magnitudes of stress concentrations in fibers neighboring a break. In the remainder of this paper we will present a model that improves upon these features in a fashion that is consistent with the finite element method and the principle of virtual work.

COMPOSITE WITH FIBERS IN A SQUARE ARRAY

Consider a unidirectional composite with fibers arranged in a perfectly square array. The spacing between the centers of nearest neighbor fibers is w. The Young's modulus of the fibers is E_f, and their diameter is D. The axial shear modulus of the matrix is G_m. Since it is assumed that the matrix does not carry axial forces, the axial Young's modulus of the matrix is zero.

Now consider a finite element representation of this composite as drawn in Figure 1. All nodes in the model are located at the fiber centers with the matrix represented by three-dimensional, anisotropic, eight noded, brick elements. Each of these elements has only eight degrees of freedom since the transverse displacements are assumed to be unimportant. Note here that this technique can naturally include the effects of transverse displacements (and stresses) if this assumption is not used. In this work the transverse displacements are neglected in order to keep the model and the governing equations as simple as possible. Let the direction parallel to the fibers be x, and the displacements in this direction be U. The transverse dimensions of the element are w by w and the length of the element in the x direction is Δx. For the simple geometry considered the stiffness of a matrix element can be derived from the finite element formulation in closed form. The interpolation uses a trilinear function in coordinates x, y, and z to determine the distribution of U within each finite element consistent with the values of U at the nodes [9]. The fibers are represented by one-dimensional axial spring elements with stiffness

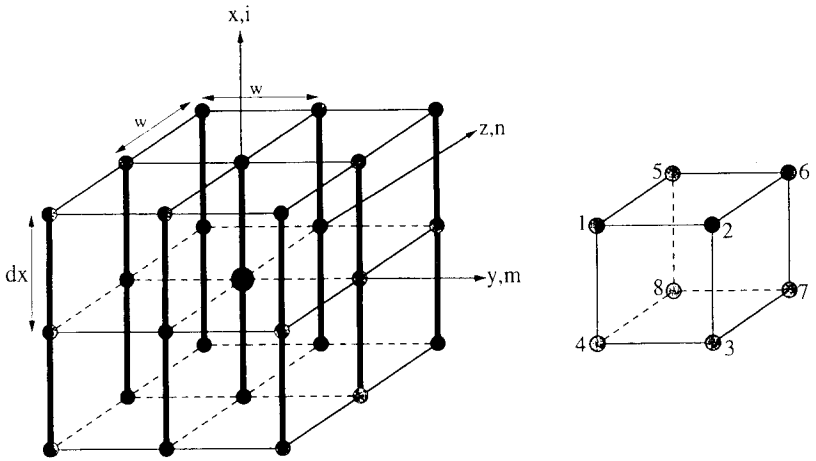

Figure 1. *The mesh and element numbering for the square fiber array.*

$$\frac{\pi D^2 E_f}{4\Delta x}$$

and these springs connect neighboring nodes along the fiber line. This geometry provides a finite element model which has axial spring elements connecting nodes along a single fiber and three-dimensional matrix elements connecting fibers to their nearest and next nearest neighbors. The finite element equation representing this set up for the typical node shown in Figure 1 is

$$\begin{aligned}
&8K_{11}U_{m,n,l} + [K_{12} + K_{34} + K_{56} + K_{78}](U_{m+1,n,l} + U_{m-1,n,l}) \\
&+ [K_{15} + K_{26} + K_{37} + K_{48}](U_{m,n+1,l} + U_{m,n-1,l}) \\
&+ [K_{14} + K_{23} + K_{58} + K_{67}](U_{m,n,l+1} + U_{m,n,l-1}) \\
&+ [K_{24} + K_{68}](U_{m+1,n,l+1} + U_{m-1,n,l-1}) \\
&+ [K_{13} + K_{57}](U_{m+1,n,l-1} + U_{m-1,n,l+1}) \\
&+ [K_{16} + K_{47}](U_{m+1,n+1,l} + U_{m-1,n-1,l}) \\
&+ [K_{25} + K_{38}](U_{m+1,n-1,l} + U_{m-1,n+1,l}) \\
&+ [K_{36} + K_{45}](U_{m,n+1,l+1} + U_{m,n-1,l-1}) \\
&+ [K_{18} + K_{27}](U_{m,n+1,l-1} + U_{m,n-1,l+1}) \\
&+ K_{17}(U_{m+1,n+1,l-1} + U_{m-1,n-1,l+1}) \\
&+ K_{28}(U_{m-1,n+1,l-1} + U_{m+1,n-1,l+1}) \\
&+ K_{35}(U_{m-1,n+1,l+1} + U_{m+1,n-1,l-1}) \\
&+ K_{46}(U_{m+1,n+1,l+1} + U_{m-1,n-1,l-1}) = 0
\end{aligned} \tag{1}$$

where the subscripts m, n and i represent the discretized node numberings in the y, z and x directions as shown in Figure 1, and K_{ij} is the force on node i when node j is displaced by a unit distance and all other nodes, including node i, have zero displacement. Using the finite element formulation described in Reference [9] the K_{ij} for the brick element including the spring elements are

$$K_{11} = \frac{E_f(\pi D^2)}{16\Delta x} + \frac{2}{9}G_m\Delta x \tag{2a}$$

$$K_{12} = K_{34} = K_{56} = K_{78} = K_{15} = K_{26} = K_{37} = K_{48} = -\frac{1}{18}G_m\Delta x \tag{2b}$$

$$K_{13} = K_{18} = K_{27} = K_{57} = K_{24} = K_{68} = K_{36} = K_{45} = -\frac{1}{36}G_m\Delta x \tag{2c}$$

$$K_{14} = K_{23} = K_{58} = K_{67} = -\frac{E_f(\pi D^2)}{16\Delta x} + \frac{1}{9}G_m\Delta x \tag{2d}$$

$$K_{16} = K_{25} = K_{38} = K_{47} = -\frac{1}{9}G_m\Delta x \tag{2e}$$

$$K_{17} = K_{28} = K_{35} = K_{46} = -\frac{1}{18}G_m\Delta x \tag{2f}$$

Note that the stiffness per unit length of an element is G_m when it is subjected to a uniform shear deformation.

It is now possible to make this model continuous in the x direction by dividing Equation (1) by Δx, and taking the limit as $\Delta x \to 0$. In this limit

$$\frac{U_{m,n,i+1} - 2U_{m,n,i} + U_{m,n,i-1}}{\Delta x^2} = \frac{d^2U_{m,n}}{dx^2} \tag{3a}$$

and any U that is not divided by Δx^2 has the simplification

$$U_{m,n,i+1} + U_{m,n,i} + U_{m,n,i-1} = 3U_{m,n} \tag{3b}$$

This procedure transforms the set of finite element equations into a set of coupled,

linear, ordinary differential equations governing the axial displacements, U, of the fibers. The governing equations for a representative fiber is then

$$\frac{d^2U_{m,n}}{dx^2} + \frac{4}{3\pi}\frac{G_m}{E_f D^2}(U_{m+1,n+1} + U_{m+1,n} + U_{m+1,n-1} + U_{m,n+1}$$

$$+ U_{m,n-1} + U_{m-1,n+1} + U_{m-1,n} + U_{m-1,n-1} - 8U_{m,n}) = 0 \tag{4}$$

Equation (4) indicates that the matrix surrounding a given fiber is represented by 8 equivalent shear springs connecting the fiber to its 8 immediate neighbors. The stiffness per unit length of these shear springs is exactly $G_m/3$. This result is only valid for the uniform square array of fibers and is a consequence of the assumption that the displacement field in a square matrix element can be interpolated (using a bilinear function) from the displacements of the surrounding fibers. In a manner following the original HVD work, Equation (4) can be put into non-dimensional form by letting

$$\xi = \sqrt{\frac{4}{3\pi}}\sqrt{\frac{G_m}{E_f}}\frac{x}{D} \tag{5a}$$

and

$$u = \sqrt{\frac{4}{3\pi}}\sqrt{\frac{G_m}{E_f}}\frac{1}{\varepsilon}\frac{U}{D} \tag{5b}$$

where ε is the strain applied to the composite at $x = \pm\infty$. The resulting form of Equation (4) is

$$\frac{d^2u_{m,n}}{d\xi^2} + (u_{m+1,n+1} + u_{m+1,n} + u_{m+1,n-1} + u_{m,n+1}$$

$$+ u_{m,n-1} + u_{m-1,n+1} + u_{m-1,n} + u_{m-1,n-1} - 8u_{m,n}) = 0 \tag{6}$$

The normalized axial stress in a fiber is then given by

$$s_{m,n} \equiv \frac{\sigma_{m,n}}{E_f\varepsilon} = \frac{du_{m,n}}{d\xi} \tag{7}$$

The boundary conditions for a composite extended to strain ε with a single fiber break located at $m = 0$, $n = 0$, and $\xi = 0$ are

$$s_{0,0}(\xi = 0) = 0 \tag{8a}$$

$$u_{m,n}(\xi = 0) = 0 \text{ for } m \text{ and } n \neq 0 \tag{8b}$$

$$s_{m,n}(\xi = \infty) = 1 \text{ for all } m \text{ and } n \tag{8c}$$

As in the HVD paper the influence function technique is used to solve this mixed boundary value problem. The influence function is determined by solving a complimentary problem where a unit opening displacement is applied at the break. For this problem the boundary conditions are

$$u_{0,0}(\xi = 0) = 1 \tag{9a}$$

$$u_{m,n}(\xi = 0) = 0 \text{ for } m \text{ and } n \neq 0 \tag{9b}$$

$$s_{m,n}(\xi = \infty) = 0 \text{ for all } m \text{ and } n \tag{9c}$$

Then by using the Fourier series transformation

$$\bar{u}(\xi, \theta, \phi) = \sum_{m=-\infty}^{\infty} \sum_{n=-\infty}^{\infty} u_{m,n}(\xi) e^{-in\theta} e^{im\phi} \tag{10a}$$

with the inverse transform

$$u_{m,n}(\xi) = \frac{1}{4\pi^2} \int_{-\pi}^{\pi} \int_{-\pi}^{\pi} \bar{u}(\xi, \theta, \phi) e^{in\theta} e^{im\phi} d\theta d\phi \tag{10b}$$

the transformed equation and boundary conditions become

$$\frac{\partial^2 \bar{u}}{\partial \xi^2} + (2\cos\theta + 2\cos\phi + 4\cos\theta\cos\phi - 8)\bar{u} = 0 \tag{11a}$$

$$\bar{u}(0, \theta, \phi) = 1 \tag{11b}$$

$$\bar{u}(\infty, \theta, \phi) = 0 \tag{11c}$$

The solution is

$$\bar{u}(\xi, \theta, \phi) = \exp(-\alpha\xi) \tag{12a}$$

where

$$\alpha = \sqrt{8 - 2\cos\theta - 2\cos\phi - 4\cos\theta\cos\phi} \tag{12b}$$

Table 1.

Stress Concentrations	Nearest Neighbor	Next Nearest Neighbor
HVD Square	1.14622	1.02453
This work	1.08103	1.07642

Then the influence function that gives the fiber stress at location (m, n, ξ) due to a unit opening *load* applied at (0,0,0) is given by

$$q_{m,n}(\xi) = \frac{-\int_0^\pi \int_0^\pi \alpha \exp(-\alpha\xi)\cos n\theta \cos m\phi \, d\theta \, d\phi}{\int_0^\pi \int_0^\pi \alpha \, d\theta \, d\phi} \tag{13}$$

Notice that this influence function is defined differently than the one given by HVD. The non-dimensional stress at a location (m,n,ξ) for the problem of a composite which has a single break and which is loaded remotely is

$$s_{m,n}(\xi) = 1 + q_{m,n}(\xi) \tag{14}$$

A comparison of this work versus HVD for stress concentrations near a single break in a composite with fibers in a square array are given in Table 1.

COMPOSITE WITH FIBERS IN A HEXAGONAL ARRAY

Two different hexagonal "meshes" with six-fold symmetry were solved. The first, shown in Figure 2(a), is a "good" finite element mesh in that it fills space. The second mesh, shown in Figure 2(b), does not fill space but rather assumes that the "springs" connecting fibers to their nearest and next nearest neighbors are always given by the stiffness associated with the six pointed star. The first mesh will be referred to as the "true" mesh and the second will be the "false" mesh. In each mesh, each finite element is an 8-noded brick with its plan having the shape of a rhombus as shown in Figure 2. The finite element interpolation is carried out in the manner used for isoparametric elements [10]. The stiffness terms, K_{ij}, for the prismatic element are given in the Appendix.

The "true" mesh can be solved in closed form but the expressions are quite lengthy. The repeating unit in the "true" mesh consists of three fibers instead of one. The Fourier series transformation of the infinite set of equations results in three coupled ordinary differential equations. The solution procedure requires the solution of the eigenvectors and eigenvalues of a 3 by 3 matrix. The procedure has been discussed by Rossettos and Sakkas [11].

The "false" mesh is attractive because, like the square mesh, only one equation needs to be solved. It is expected that the results for the "false" mesh will be reasonably close to those for the "true" mesh. The governing equation for a representative fiber in the "false" mesh is

$$\frac{d^2U_{m,n}}{dx^2} + \frac{5}{9\sqrt{3}\pi}\frac{G_m}{E_f D^2}(4U_{m+1,n} + 4U_{m+1,n-1} + 4U_{m,n+1} + 4U_{m,n-1}$$

$$+ 4U_{m-1,n} + 4U_{m-1,n+1} + U_{m+1,n+1} + U_{m+1,n-2}$$

$$+ U_{m+2,n-1} + U_{m-1,n-1} + U_{m-1,n+2} + U_{m-1,n-1} - 30U_{m,n}) = 0 \qquad (15)$$

with the numbering system for fibers in the m and n directions shown in Figure 2(b). In similar fashion to the square array, the equation is non-dimensionalized by letting

$$\xi = \sqrt{\frac{5}{9\sqrt{3}\pi}}\sqrt{\frac{G_m}{E_f}}\frac{x}{D} \qquad (16a)$$

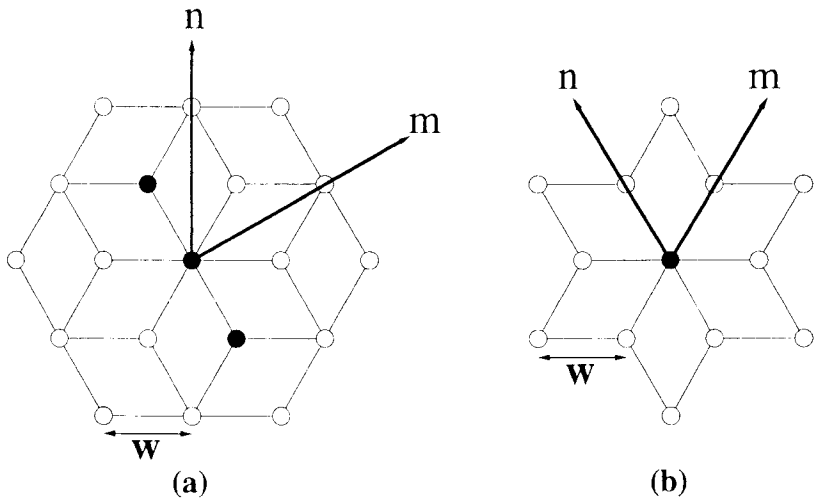

Figure 2. *(a) The "true" mesh with the shaded fibers as the repeating cell and (b) The "false" mesh with the single shaded fiber as the repeating cell.*

Table 2.

Stress Concentrations	Nearest Neighbor	Next Nearest Neighbor
True Mesh	1.085068	1.02863
False Mesh	1.08347	1.0282
HVD Hexagonal	1.10458	1.01436

and

$$u = \sqrt{\frac{5}{9\sqrt{3}\pi}}\sqrt{\frac{G_m}{E_f}}\frac{1}{\varepsilon}\frac{U}{D} \tag{16b}$$

The resulting solution and influence function are

$$\bar{u}(\xi,\theta,\phi) = \exp(-\xi\alpha) \tag{17a}$$

with

$$\alpha = \sqrt{\begin{aligned}&30 - 8\cos\theta - 8\cos\phi - 8\cos(\theta-\phi)\\&\quad - 2\cos(\theta+\phi) - 2\cos(\theta-2\phi) - 2\cos(2\theta-\phi)\end{aligned}} \tag{17b}$$

and the influence function for the fiber stress is

$$q_{mn}(\xi) = \frac{-\int_{-\pi}^{\pi}\int_{-\pi}^{\pi}\alpha\exp(-\alpha\xi)e^{in\theta}e^{im\phi}\,d\theta\,d\phi}{\int_{-\pi}^{\pi}\int_{-\pi}^{\pi}\alpha\,d\theta\,d\phi} \tag{18}$$

Table 2 compares our results from the "true" and "false" meshes to the HVD hexagonal model. It can be seen that the "true" and "false" meshes give quite similar results.

DISCUSSION AND CONCLUSION

Nedele and Wisnom [4] performed full three-dimensional finite element calculations. In the model only the broken fiber, nearest neighbor fibers, and matrix material between these fibers are modeled explicitly and the material outside of a small region beyond the nearest neighbors is represented as homogeneous transversely isotropic material. In Reference [5], Nedele and Wisnom analyze an axisymmetric finite element model of a similar system, modeling the nearest and next nearest neighbor fibers by two distinct fiber rings. Of the finite element calcula-

tions that have been done for single fiber breaks, these are the most applicable to this shear lag model because all constituents are assumed to be elastic and the fiber to matrix stiffness ratio is very high ($fE_f/(1-f)E_m \approx 90$). The high stiffness ratio gives validity to the assumption that the matrix cannot carry axial loads. In Reference [4], Nedele and Wisnom present results for the stresses at the center line of a nearest neighbor to a broken fiber in a hexagonal array. The calculations show a peak stress slightly removed from the plane of the break. The value for this stress concentration is 1.058. For the axisymmetric calculations in Reference [5] the average maximum stress concentration factor in the nearest neighbor fiber ring is 1.061. Our shear lag model does differ from this result but is in better agreement than other existing models. Two possible improvements to our model that might lead to closer results to those in References [4] and [5] would be to include the effects of axial matrix stiffness and transverse degrees of freedom. In general, the HVD model, which only connects fibers directly to their nearest neighbors and not to the next nearest neighbors, yields values for stress concentrations that are high for the nearest neighbor and low for the next nearest neighbor. This is especially pronounced in the square array where the next nearest neighbor is still relatively close to the broken fiber.

The idea of representing the matrix by three-dimensional finite elements is not a new one. Cox et al. [12] formulated what is called the binary model to handle the complicated geometries of woven composites. This model uses one-dimensional axial spring elements to represent the fibers, and three-dimensional "effective medium" elements to represent the matrix and transverse properties of the fibers. This model has been used by McGlockton et al. [13,14] to study failure of woven composites and the failure of unidirectional composites.

The model presented here takes the finite element approach one step further to make the model smooth and continuous in the fiber direction rather than piecewise continuous. The only assumptions made about the matrix are that it does not carry axial load, and that the displacements in the matrix can be interpolated from the displacements of the fibers surrounding it. Once this is done, as in conventional finite elements, the principle of virtual work is used to find the minimum energy configuration for the fiber displacements. In the problem presented here, degrees of freedom are assigned to the fibers. Once the displacements along the fibers are known the displacement field in the matrix can be found using the interpolation functions. Neglecting any rigid body translation, this displacement field gives rise to deformation and stress in the fibers and matrix. The principle of virtual work is used to ensure that the solution to the problem (in fact to any finite element problem) is the one that yields the minimum total energy in the system. For the system considered here the total energy includes the strain energy stored in the fibers and matrix, and the work done by the applied loads.

The usefulness of this model is in its applications to problems beyond the stress concentrations around a single fiber break. The model is a building block for

studying the failure of unidirectional fiber composites and the influence functions presented here are the critical component in the break influence superposition technique (Sastry and Phoenix, [7]) which can be used to address such problems. In subsequent papers Landis and McMeeking [15] use the finite element methodology to include the effects of interface sliding, axial matrix stiffness, and uneven fiber positioning on stress concentrations around a single fiber break, and Landis et al. [16] use the formulation presented in this paper to simulate the failure of well bonded fiber composites. Furthermore, this methodology presents a consistent framework for analyzing composite failure mechanisms at the micro or constituent level.

ACKNOWLEDGEMENT

The work was sponsored by the Advanced Research Projects Agency through the University Research Initiative at the University of California, Santa Barbara (ONR Contract N-0014-92-J-1808).

APPENDIX: PRISMATIC ELEMENT STIFFNESS

The node numbering for the prismatic element is shown in Figure A1. The stiffnesses for the element including the contributions from the fiber spring elements are:

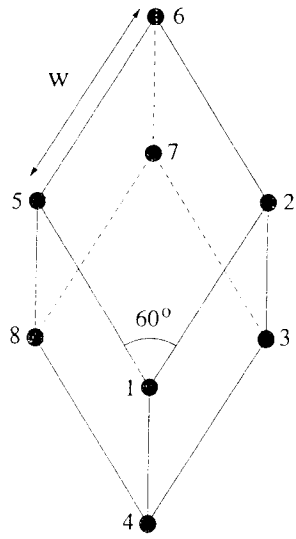

Figure A1. *The element shape and node numbering used for the hexagonal models.*

$$K_{11} = K_{44} = K_{66} = K_{77} = \frac{E_f(\pi D^2)}{24\Delta x} + \frac{5}{18\sqrt{3}} G_m \Delta x \tag{A1}$$

$$K_{22} = K_{33} = K_{55} = K_{88} = \frac{E_f(\pi D^2)}{12\Delta x} + \frac{11}{18\sqrt{3}} G_m \Delta x \tag{A2}$$

$$K_{12} = K_{34} = K_{56} = K_{78} = K_{15} = K_{26} = K_{37} = K_{48} = -\frac{1}{9\sqrt{3}} G_m \Delta x \tag{A3}$$

$$K_{13} = K_{18} = K_{27} = K_{57} = K_{24} = K_{68} = K_{36} = K_{45} = -\frac{1}{18\sqrt{3}} G_m \Delta x \tag{A4}$$

$$K_{14} = K_{67} = -\frac{E_f(\pi D^2)}{24\Delta x} + \frac{5}{36\sqrt{3}} G_m \Delta x \tag{A5}$$

$$K_{23} = K_{58} = -\frac{E_f(\pi D^2)}{12\Delta x} + \frac{11}{36\sqrt{3}} G_m \Delta x \tag{A6}$$

$$K_{16} = K_{47} = -\frac{1}{18\sqrt{3}} G_m \Delta x \tag{A7}$$

$$K_{25} = K_{38} = -\frac{7}{18\sqrt{3}} G_m \Delta x \tag{A8}$$

$$K_{17} = K_{46} = -\frac{1}{36\sqrt{3}} G_m \Delta x \tag{A9}$$

$$K_{28} = K_{35} = -\frac{7}{36\sqrt{3}} G_m \Delta x \tag{A10}$$

REFERENCES

1. Hedgepeth, J. M. 1961. "Stress Concentrations in Filamentary Structures," *NASA TN D-882.*
2. Hedgepeth, J. M. and P. van Dyke. 1967. "Local Stress Concentrations in Imperfect Filamentary Composite Materials," *J. Compos. Mater.*, 1:294–309.
3. Beyerlein, I. J., S. L. Phoenix and A. M. Sastry. 1996. "Comparison of Shear-Lag Theory and Continuum Fracture Mechanics for Modeling Fiber and Matrix Stresses in an Elastic Cracked Composite Lamina," *Int. J. Solids Structures*, 33:2543–2574.

4. Nedele, M. R. and M. R. Wisnom. 1994. "Three-Dimensional Finite Element Analysis of the Stress Concentration at a Single Fibre Break," *Comp. Sci. Technol.*, 51:517–524.
5. Nedele, M. R. and M. R. Wisnom. 1994. "Stress Concentration Factors Around a Broken Fiber in a Unidirectional Carbon Fibre-Reinforced Epoxy," *Composites*, 7:549–557
6. Cox, H. L. 1952. "The Elasticity and Strength of Paper and Other Fibrous Materials," *Br. J. Appl. Phys.*, 3:72.
7. Sastry, A. M. and S. L. Phoenix. 1993. "Load Redistribution Near Non-Aligned Fiber Breaks in a Two Dimensional Unidirectional Composite Using Break Influence Superposition," *J. Mater. Sci. Lett.*, 12:1596–1599.
8. Beyerlein, I. J. and S. L. Phoenix. 1997. "Statistics of Fracture for an Elastic Notched Composite Lamina Containing Weibull Fibers—Part I. Features from Monte-Carlo Simulation, *Eng. Frac. Mech.*, 57:241–265.
9. Cook, R. D., D. S. Malkus and M. E. Plesha. 1974. *Concepts and Applications of Finite Element Analysis*. Third Edition, John Wiley & Sons.
10. Irons, B. M. 1966. "Engineering Applications of Numerical Integration in Stiffness Methods." *AIAA Jnl.*, 4(11):2035–2037.
11. Rossettos, J. N. and K. Sakkas. 1991. "Effect of Fiber Modulus Variations on Stress Concentration in Hybrid Composites," *AIAA Jnl.*, 29(3):482–484.
12. Cox, B. N., W. C. Carter and N. A. Fleck. 1994. "A Binary Model of Textile Composites—I. Formulation," *Acta Metall. Mater.*, 42(10):3463–3479.
13. McGlockton, M. A., R. M. McMeeking and B. N. Cox. 1997(a). "A Model for the Axial Strength of Unidirectional Ceramic Matrix Fiber Composites." To be published.
14. McGlockton, M. A., R. M. McMeeking and B. N. Cox. 1997(b). "A Model for the Tensile Failure of 3-D Woven Textile Composites," To be published.
15. Landis, C. M. and R. M. McMeeking. 1998. "Stress Concentrations in Composites, with Interface Sliding, Matrix Stiffness, and Uneven Fiber Spacing Using Shear Lay Theory," to appear in *Int. J. Solids Struct.*
16. Landis, C. M., I. J. Beyerlein and R. M. McMeeking. 1998. "Micromechanical Simulation of the Failure of Fiber Reinforced Composites," submitted to *J. Mech. Phys. Solids.*